NOAA TECHNICAL REPORT NWS/NCEP 99-01

# Documentation of Version 2 of Relaxed Arakawa-Schubert Cumulus Parameterization with Convective Downdrafts

Camp Springs, MD
June 1999

**U.S. DEPARTMENT OF COMMERCE**
**National Oceanic and Atmospheric Administration**
National Weather Service

NOAA TECHNICAL REPORT NWS/NCEP 99-01

# Documentation of Version 2 of Relaxed Arakawa-Schubert Cumulus Parameterization with Convective Downdrafts

Shrinivas Moorthi
Environmental Modeling Center
National Centers for Environmental Prediction
National Weather Service
Camp Springs, Maryland 20746

Max J. Suarez
National Aeronautics and Space Administration
Goddard Space Flight Center
Greenbelt, Maryland 20771



June 1999

**U.S. DEPARTMENT OF COMMERCE**
**William M. Daley, Secretary**
**National Oceanic and Atmospheric Administration**
D. James Baker, Under Secretary
National Weather Service
John J. Kelly, Jr., Assistant Administrator

## Abstract

A documentation of a revised version of the Relaxed Arakawa-Schubert (RAS) convection parameterization is presented. This version includes several important improvements of the original RAS described in Moorthi and Suarez (1992). The cloud model now accounts for virtual effects of moisture in the buoyancy calculations. It also includes suspended condensate loading and autoconversion at various levels, producing precipitation as a function of height. The suspended condensate is detrained at the cloud-top and can be used as a source term for models with prognostic cloud condensate. A simple treatment of the ice phase has also been added.

Following the approach of Cheng and Arakawa (1997a,b), a scheme for the evaporatively driven convective downdraft is included. An additional scheme, following Sud and Molod (1988), to account for the evaporation of the falling rain that does not generate downdrafts, is also included.

Results from semi-prognostic tests with GATE data are presented. It is found that, without the downdraft, the new version of RAS produces results comparable to those for the original RAS, with excessive heating and drying. Inclusion of the downdraft reduces both the heating and drying. Results are also sensitive to whether the convective subsidence is allowed to directly modify the subcloud layer or not.

# 1 Introduction

Cumulus convection plays a dominant role in both the thermodynamical and the hydrological cycles of the earth's atmosphere. Accurate prediction of heat and moisture changes in the atmosphere due to cumulus convection is crucial to the success of numerical weather prediction, as well as to climate and global change studies. The most elegant and complete theory of the interaction between cumulus ensembles and the large-scale environment is presented in the pioneering work of Arakawa and Schubert (1974, hereafter AS), and has remained so for over two decades. Nevertheless, the standard implementation of this theory in weather prediction and climate models (e.g., Lord et al., 1982) is quite expensive, particularly when the vertical resolution is high. This has limited the application of the AS scheme.

The AS parameterization assumes that convection will act to maintain the atmospheric sounding in a state of "quasi-equilibrium" in which the tendency of other (slower) processes to destabilize the sounding are closely compensated by the tendency of the convection to stabilize it. In AS the assumption that this state obtains at each instant, together with some simple assumptions about the interactions between individual clouds and the environment—the so-called "cloud model"—is sufficient closure to compute the vertical profiles of heating and moistening due to the effects of convection. AS, however, says nothing about how this adjustment takes place, other than that it should occur quickly compared to changes in the destabilizing effects of the large-scale flow.

Moorthi and Suarez (1992, hereafter, MS) developed the relaxed Arakawa-Schubert (RAS) scheme, which is a simple and economical implementation of the basic ideas of AS. It is based on the notion that the adjustment required by AS can be effected in a finite time. In developing RAS, MS made several simplifications, both in the cloud model and in the manner in which quasi-equilibrium is achieved. The cloud model was simplified by assuming that the normalized cloud updraft mass flux is a linear function of height and by ignoring the effects of cloud condensate loading and moisture content in the buoyancy calculations. The quasi-equilibrium is achieved through an iteration that "relaxes" the sounding toward the equilibrium state in a prescribed

time, instead of simultaneously letting all cloud ensembles adjust the environment to a state of equilibrium (as in the AS implementation). The iteration is performed by adding at each step the effects of a single cloud type. In practice, this is achieved by invoking several cloud types every time step, one by one, and letting a fraction (the relaxation parameter) of the mass flux required for full quasi-equilibrium modify the environment. Thus, the computation of effects of these individual cloud types is the core of the RAS calculation.

RAS has been quite successful in achieving its original goals of economy and simplicity while retaining the essence of AS, and some form of it is being used at several institutions. However, as in the original implementation of AS, RAS suffers from excessive drying due to the lack of downdraft effects as well as to a lack of evaporation of falling rain in the environment. A method for reducing the excessive drying was proposed by Sud and Molod (1988) in their implementation of AS. Moorthi (1999) included a simplified version of the Sud and Molod scheme for evaporation of falling convective rain to alleviate this excessive dry and warm bias in the original RAS. Sud and Walker (1999a,b) developed a methodology to couple microphysics of clouds with RAS and included a downdraft scheme based on Sud and Walker (1993).

In this report we present an advanced version of RAS in which several simplifications made in the original RAS are removed. The major changes are in the cloud updraft model. It now includes a budget of condensed water within the clouds. This allows the inclusion of condensate loading in the computation of the buoyancy. Since the buoyancy calculation was thus significantly altered, we also took the opportunity to include the virtual effect of water vapor, which had been omitted in MS. Finally, we also allow for the normalized mass flux to be a quadratic function of height to alleviate problems associated with the linear mass flux used in MS, and have included a simple ice phase. These additions give us a fairly complete implementation of the AS updraft cloud model and should greatly facilitate the coupling of the updraft to downdraft and stratiform cloud schemes.

Recently Cheng and Arakawa (1997a, 1997b, hereafter CA97a and CA97b) have presented a formulation of convective downdrafts and applied it to the standard implementation of AS. There are several attractive features in this downdraft formulation.

Downdrafts are driven by precipitation loading and evaporation. Downdrafts can be saturated or unsaturated and no assumption is made in this regard. The precipitation flux that is available for the downdraft is obtained as a steady state solution of a tilted updraft. Thus, the precipitation need not be available for the downdraft at the level where it is generated, and can be vertically advected within the updraft. Downdrafts can start and end anywhere in the vertical domain. However, both the scheme for the determination of the available rain flux from the updraft and the calculation of the downdraft properties are computationally intensive. Nevertheless, we have incorporated a version of this downdraft scheme with some approximations in the present version of RAS.

The organization of the document is as follows. In Section 2 some basic relations are reviewed. In Section 3 we present details of the new cloud updraft model. In Section 4 we discuss our implementation of the Cheng and Arakawa (hereafter, CA) downdraft formulation. In section 5 modification of the large-scale environment is discussed. In section 6 the vertically discrete formulation is given. In Section 7 we present results from a semi-prognostic evaluation using GATE Phase III data. A strategy for application of the parameterization to numerical models of the atmosphere with high vertical resolution is presented in Section 8. A summary is provided in Section 9. Some additional details of the parameterization are provided in the Appendix A. A scheme for evaporation of falling precipitation is given in Appendix B.

# 2 Basic Relations

Treating moist air as an ideal gas, the equation of state is

$$p = \left( \frac{\rho_d}{\mu_d} + \frac{\rho_\mathrm{v}}{\mu_\mathrm{v}} \right) R^* T = \rho R_d T_\mathrm{v}, \tag{1}$$

where $p$ is the pressure, $\mu_d = 28.97$ and $\mu_\mathrm{v} = 18.016$ are the molecular weights of dry air and water vapor, $R^*$ is the universal gas constant, $R_d = \frac{R^*}{\mu_d}$ is the gas constant for dry air, $\rho_d$ and $\rho_\mathrm{v}$ are the densities of dry air and water vapor, $\rho = \rho_d + \rho_\mathrm{v}$ is the

density of the moist air, $T$ is the temperature, and

$$T_{\rm v} = [1 + (\frac{\mu_d}{\mu_{\rm v}} - 1)q\,]\,T = (1 + \nu q)\,T \tag{2}$$

is the virtual temperature, $q = \frac{\rho_{\rm v}}{\rho}$ being the specific humidity. We have defined the constant $\nu \equiv (\frac{\mu_d}{\mu_{\rm v}} - 1) \approx 0.608$.

The new RAS also uses the same form of the hydrostatic equation as the Arakawa and Suarez (1983) scheme, but with virtual effects of moisture:

$$d\phi = -\theta_{\rm v}\, d\Pi, \tag{3}$$

where $\phi = gz$ is the geopotential, $z$ is height, $g$ is the acceleration of gravity, $\theta_{\rm v} = c_p \frac{T_{\rm v}}{\Pi}$ is the virtual potential temperature, $\Pi = c_p \left(\frac{p}{p_o}\right)^{\kappa}$ is the Exner function, $p_o$ is a reference pressure, $c_p$ is the specific heat of dry air at constant pressure, and $\kappa = R_d/c_p$.

We define the dry static energy, $s$, the moist static energy, $h$, and the saturated moist static energy, $h^*$, as

$$s = c_p T + \phi, \tag{4a}$$

$$h = s + L_c q, \tag{4b}$$

$$h^* = s + L_c q^*, \tag{4c}$$

where $L_c$ is the latent heat of condensation of water vapor, which is assumed to be a constant, and $q^* = q_{sat}(T, p)$ is the saturation specific humidity. The dry static energy is conserved during a dry adiabatic process, and the moist static energy is conserved during a pseudo-adiabatic process not involving the ice phase. When the ice phase is involved, a generalized moist static energy defined as

$$h = s + L_c q - L_f q^I \tag{5}$$

is conserved (Lord, 1978), where $q^I$ is the specific mass of ice water, and $L_f$ is the latent heat of fusion of water. Another conservative quantity is the total specific mass of water, $q^T$, defined as

$$q^T = q + q^L + q^I, \tag{6}$$

where $q^L$ is the specific mass of liquid water. In the present formulation of RAS we allow for ice phase condensate by using a simple partitioning similar to that used by Lord (1978). Thus we approximate

$$q^I = Q(T)q^C \tag{7}$$

where $q^C = q^L + q^I$ is the total condensate, and $Q(T)$ is a temperature dependent function, defined as

$$Q(T) = \frac{T_L - T}{T_L - T_F} \tag{8}$$

where $T_L = -263.16\ K$, $T_F = -233.16\ K$, and $0 \leq Q \leq 1$ is required. In Lord (1978), $T$ was taken as the temperature of the cloud air, but for simplicity we use the environmental temperature.

The virtual dry static energy $s_{\rm v}$ is defined as

$$s_{\rm v} = s + c_p T(\nu q - q^L - q^I). \tag{9}$$

It will be convenient also to define the quantity

$$\gamma = \frac{L_c}{c_p}\frac{\partial q^*}{\partial T}(T, p). \tag{10}$$

# 3 The Updraft Cloud Model

Deep cumulus clouds are assumed to consist of a saturated updraft, possibly accompanied by a downdraft. The entire cloud is assumed to occupy a small horizontal area. Subsidence that exactly compensates the net updraft and downdraft mass fluxes is assumed to occur uniformly in the large-scale environment outside the cloud. This subsidence produces the heating and drying effects of the clouds on the environment. In this section we discuss the updraft model.

## 3.1 Updraft Properties

The updraft mass flux, $M^u$, is written as

$$M^u(z) = M_B\,\eta^u(z), \tag{11}$$

where $M_B$ is the mass flux entering the updraft at cloud base, $z_B$, and $\eta^u(z)$ is the normalized mass flux as a function of height; obviously, $\eta^u(z_B) = 1$. (We will use the superscript "$u$" to denote updraft properties. The absence of a superscript indicates environmental properties.) Within the updraft, the divergence of the flux of conservative quantities must equal the entrainment flux. Mass conservation is thus written as

$$d\eta^u = \mathcal{E}\,dz, \tag{12}$$

where $\mathcal{E}$ is the normalized lateral mass entrainment per unit height. Using the generalized moist static energy, $h$, and total specific mass of water, $q^T$, as the two conservative thermodynamic quantities, we write

$$d(\eta^u h^u) = h\mathcal{E}\,dz = h\,d\eta^u, \tag{13}$$

for the moist static energy budget, and

$$d(\eta^u q^{uT}) = q^T\mathcal{E}\,dz - \mathcal{R}\,dz = q^T\,d\eta^u - \mathcal{R}\,dz, \tag{14}$$

for the total water budget, where $h$ and $q^T$ represent moist static energy and total specific mass of water in the environment, $\mathcal{R}$ is the precipitation production rate per unit height normalized by $M_B$, and

$$h^u = c_pT^u + \phi + L_cq^u - L_fq^{uI} \tag{15}$$

is the generalized moist static energy in the cloud updraft, where

$$q^u = q^{uT} - q^{uL} - q^{uI}. \tag{16}$$

Here $q^u$, $q^{uT}$, $q^{uL}$, and $q^{uI}$ are the cloud updraft specific humidity, total specific mass of water, specific mass of liquid water, and specific mass of ice, respectively. In (13) and (14) we have assumed that all lateral entrainment into the updraft is from the

environment and none is from the associated downdraft. The total specific water in the entrained air is $q^T = q + q^L + q^I$ if the environment contains suspended liquid water and/or ice. Integrating (13) and (14) gives

$$\eta^u(z)h^u(z) = h_B + \int_{z_B}^{z} h(z')\frac{d\eta^u}{dz'}\,dz', \tag{17}$$

and

$$\eta^u(z)q^{uT}(z) = q_B + \int_{z_B}^{z} q^T(z')\frac{d\eta^u}{dz'}\,dz' - \int_{z_B}^{z} \mathcal{R}\,dz', \tag{18}$$

since the subcloud layer is assumed to be unsaturated. Here $z$ is height and the subscript "$B$" represents values at the top of the subcloud layer.

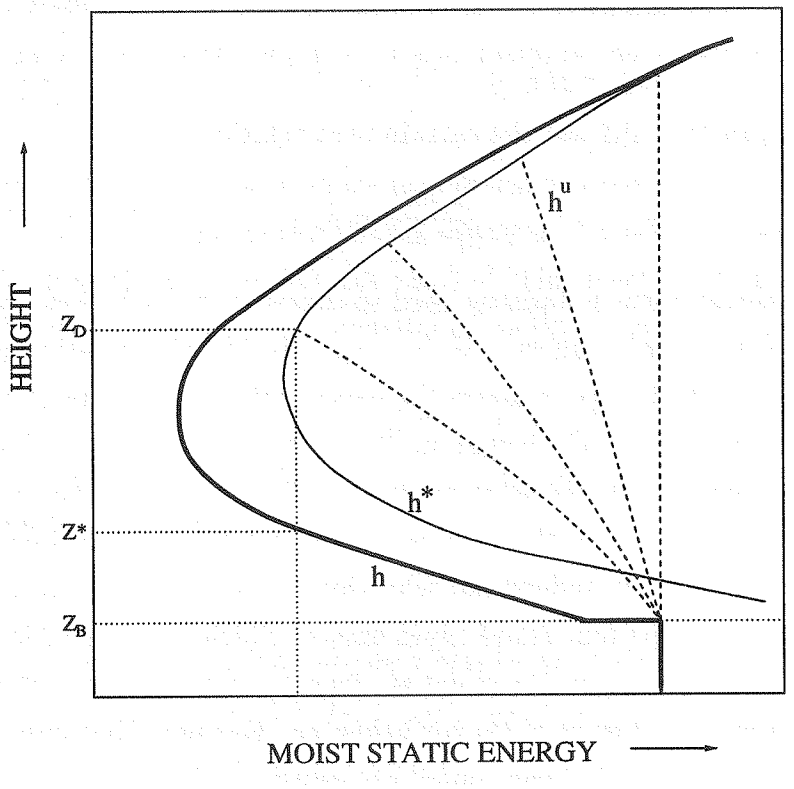


Figure 1: Schematic of the moist static energy distributions.

Figure 1 shows schematically the vertical profile (thick solid line) of moist static energies that occur typically in a conditionally unstable sounding. The subcloud layer

is shown as a mixed layer with constant $h$. The sounding is unsaturated everywhere, with $h < h^*$. The dashed lines show four possible distributions of updraft moist static energy, $h^u$, corresponding to four different rates of entrainment. As can be seen from (17), $h^u(z)$ is a weighted average of the $h$ in the subcloud layer and in the environment at levels below $z$.

## 3.2 The Entrainment Relation

In the AS parameterization, cloud types are characterized completely by their rate of lateral entrainment. The higher the rate of entrainment, the closer $h^u$ is to the environmental value $h$, and as can be seen from figure 1, the lower the level at which $h^u = h^*$. This is approximately the level of non-buoyancy and usually assumed to be the cloud top. A higher entrainment rate thus implies shallower clouds.

As is standard practice, AS use the entrainment relation

$$\frac{1}{\eta^u}\frac{d\eta^u}{dz} = \lambda, \tag{19}$$

where $\lambda$ is the entrainment parameter used to characterize each cloud type. Integrating (19) gives $\eta^u(\tilde{z}) = e^{\lambda\tilde{z}}$, where $\tilde{z} = (z - z_B)$. In MS this relation was simplified to $\eta^u(\tilde{z}) = 1 + \lambda\tilde{z}$, which approximates the exponential only for small $\lambda\tilde{z}$ and implies constant entrainment per unit height in the vertical. Arakawa and Cheng (1993) noted that this approximation systematically reduces the occurrence of soundings that can support middle level cloud types, whose detrainment level is near the level of minimum $h$ and $h^*$. To understand why this is, we again refer to figure 1. If we consider the lowest of the four cloud types shown, which detrains at level $z_D$, we see that the moist static energy in the cloud at cloud top must be near $h^*(z_D)$ and must be obtained through a mixture of the air below $z_D$. But note that only the relatively small region between $z_D$ and $z^*$ can contribute values of $h$ lower than $h^*(z_D)$; while the larger region below $z^*$ contributes air with moist static energies greater than $h^*(z_D)$, particularly if the lower atmosphere is relatively moist. For linear entrainment, as assumed in MS, these two contributions would receive roughly equal weight. As a result, it is virtually impossible to find a $\lambda$ that yields $h^u(z_D) \approx h^*(z_D)$. In fact,

$h^u$ at any level below the minimum in $h^*$ cannot be less than the height-averaged environmental $h$ between that level and cloud base. For entrainment that increases exponentially with height, the upper contribution could receive a much greater weight, and it would thus be more likely that a $\lambda$ could be found that produces a mixture yielding $h^u(z_D) \approx h^*(z_D)$. Thus, entrainment that rapidly increases with height is essential for the existence of shallow cloud types.

To more closely approximate the behavior of the original AS scheme, while retaining most of the efficiency of the linear $\eta^u$ relation, the new version of RAS uses a quadratic relation:

$$\eta^u(\tilde{z}) = 1 + \lambda\tilde{z} + \frac{1}{2}(\lambda\tilde{z})^2. \tag{20}$$

As we shall see below, this can be implemented with little additional calculation.

## 3.3 Buoyancy and the Cloud Work Function

In this version of RAS, we use a more precise calculation of the buoyancy of the updraft than used in MS, including virtual effects and loading by suspended cloud condensate (both water and ice, but not rain). [1] The acceleration due to buoyancy of an updraft parcel consisting of a mixture of moist air and suspended condensed water is

$$B^u = -g\frac{\rho^u - \rho}{\rho^u} - g[q^{uL} + q^{uI} - q^L - q^I], \tag{21}$$

where $\rho^u$ is the density of moist air within the updraft and $\rho$ is the density of moist air in the environment.

Using (1) and neglecting density variations due to pressure differences between the updraft and the environment, the buoyancy can be accurately approximated by

$$B^u = g\left[\frac{T_{\rm v}^u - T_{\rm v}}{T_{\rm v}} - q^{uL} - q^{uI} + q^L + q^I\right]. \tag{22}$$

Now

$$T_{\rm v}^u - T_{\rm v} = (T^u - T)(1 + \nu q^*) + \nu T(q^u - q^*) + \nu T(q^* - q) + \nu(T^u - T)(q^u - q^*). \tag{23}$$

[1] The impact of precipitation within the updraft itself would be to reduce the updraft buoyancy thus inhibiting the cloud's growth and leading to its destruction. Nevertheless, we do not take into account this drag in calculating the buoyancy of the updraft.

Ignoring the last quadratic term and using the following approximate relations

$$T^u - T = \frac{1}{c_p(1+\gamma)}[h^u + L_f q^{uI} - h^*], \tag{24}$$

and

$$q^u - q^* = \frac{\gamma}{L_c(1+\gamma)}[h^u + L_f q^{uI} - h^*], \tag{25}$$

which are valid for a saturated parcel, we can write the buoyancy above the condensation level in the form

$$B^u = \frac{g}{\tilde{L}}\left[h^u + L_f q^{uI} - h^{**} - \tilde{L}(q^{uL} + q^{uI} - q^L - q^I)\right], \tag{26}$$

where, similarly to CA97b, we have defined a grid-scale virtual moist static energy $h^{**}$ as

$$h^{**} = h^* - \frac{\nu\tilde{L}}{(1+\nu q^*)}[q^* - q], \tag{27}$$

and

$$\tilde{L} = \frac{(1+\gamma)c_p T_{\mathrm{v}}}{(1+\gamma\nu c_p T/L)}. \tag{28}$$

Below the condensation level, the buoyancy can be approximated by

$$B^u = \left[\frac{(s^u - s)}{c_p T_{\mathrm{v}}} + \nu(q^u - q) + q^L + q^I\right]. \tag{29}$$

Following AS, we define the cloud work function as the work done by thermal buoyancy of the updraft per unit cloud-base mass flux:

$$\mathcal{A} \equiv \int_{z_B}^{z_D} \eta^u(z) B^u(z)\, dz. \tag{30}$$

Here $z_D$ is the height of the cloud top. CA97a have provided alternate definitions of the cloud work function for combined updraft-downdraft models by taking into account rain-water drag on updraft, and thermal buoyancy and rain-water drag in the downdraft. CA97a showed that despite the differences in magnitude of the cloud work function with these alternate definitions, they are proportional to each other and that using the definition (30) in implementing cloud work function quasi-equilibrium is acceptable. Following their lead, we also use (30) in our implementation, since this results in significant savings in computations.

Combining (30) with (29) and (26) gives

$$\mathcal{A} \approx g\int_{z_B}^{z_C}\left[\frac{(s^u-s)}{c_pT_v}+\nu(q^u-q)+q^L+q^I\right]\eta^u(z)\,dz + g\int_{z_C}^{z_D}\frac{1}{\tilde{L}}\left[h^u+L_fq^{uI}-h^{**}-\tilde{L}(q^{uL}+q^{uI}-q^L-q^I)\right]\eta^u(z)\,dz, \quad (31)$$

where $z_C$ is the condensation level.

## 3.4 Condensed Water/Ice Budget and the Entrainment Parameter

To compute the suspended condensate (liquid water plus ice) in the updraft, $q^{uC} = q^{uL} + q^{uI}$, we need to parameterize the rain rate, $\mathcal{R}$, in the total water budget (14). We parameterize $\mathcal{R}$ as

$$\mathcal{R} = c_o\eta^u(z)q^{uC}(z), \quad (32)$$

where $q^{uC}(z)$ is the total condensate (excluding rain water) at height $z$ in the updraft and $c_o$ is an auto conversion coefficient [2] (see Lord, 1978). Then the differential equation governing the vertical distribution of the condensate can be written as

$$\frac{d(\eta^u q^{uC})}{dz}+c_o\eta^u(z)q^{uC}(z)=q^T(z)\frac{d\eta^u}{dz}-\frac{d(\eta^u q^u)}{dz}. \quad (33)$$

Using (25), (8), and (17), (33) can, in principle, be solved to obtain the suspended liquid water at any level in the form

$$\eta^u(z)q^{uC}(z)=\lambda^2F(z)+\lambda G(z)+H(z), \quad (34)$$

where $F$, $G$, and $H$ are vertical integrals depending on environmental variables only. We provide the form of these functions for the discrete case in Section 6.

To determine the entrainment parameter, we use the non-buoyancy condition. We assume that the cloud updraft detrains at the cloud top, $z_D$, and this is the level of

[2] The auto conversion coefficient $c_o$ can be a function of height or temperature. For the results presented in this report we used $c_o$=0.002. To use different values for water and ice one could easily replace $c_o$ in (32) by $c_o = (1-Q(T))c_{ow} + Q(T)c_{oI}$ where $c_{ow}$ and $c_{oI}$ are the auto conversion coefficients for water and ice, respectively.

non-buoyancy. Using the form of the buoyancy that appears in the integrand of (31) for levels above $z_C$, we find the following condition at the cloud top:

$$h^u(z_D) + L_f q^{uI}(z_D) - h^{**}(z_D) - \tilde{L}(z_D)[q^{uC}(z_D) - q^C(z_D)] = 0. \tag{35}$$

This relation involves only three updraft quantities, $h^u$, $q^{uC}$, and $q^{uI}$, all evaluated at the detrainment level. The moist static energy, $h^u$, can be obtained from (17) and $q^{uC}$ from (34) using (7) for $q^{uI}$. As mentioned before, we use environmental temperature $T$ in evaluating $Q(T)$ in (7) instead of updraft temperature $T^u$. Without this simplification the entrainment parameter can only be obtained iteratively. Since the updraft air is typically a few degrees warmer than the environmental air, the above simplification would overestimate the fraction of ice in the total condensate. A crude correction can be made by reducing $T_L$ and $T_F$ in (8) by a few degrees. Nevertheless, we do not expect the error due to this approximation to be of significance since the nature of $Q(T)$ is itself quite arbitrary.

Multiplying (35) by $\eta^u(z_D)$ and using (34) and (7), we can also simplify the non-buoyancy condition into the form of a quadratic equation in the entrainment parameter $\lambda$. The three coefficients of this quadratic equation are functions of environmental variables and thus can be calculated directly. This equation provides two solutions for $\lambda$. We choose the larger real positive solution if it exists. If no real positive solution exists, we assume that such a cloud type cannot exist. Once $\lambda$ is known, we can obtain the vertical profiles of $q^{uC}$, $q^{uI}$, $h^u$, etc. Again, the details are provided in Section 6 for the discrete case.

# 4 The Cheng and Arakawa Downdraft

In this report we document the simplified version of the CA downdraft formulation (Cheng, 1989, CA97a, CA97b) applied to RAS. We will focus on the RAS implementation of the downdraft and give only a brief summary of other details, since they are available in the above references. In CA the rain generated in the updraft may remain in the updraft or fall outside of the updraft. The rain that falls outside of the updraft can produce convective scale downdrafts through evaporation and fric-

tional drag. Thus, the CA downdraft formulation has two major steps. The first step involves the determination of steady-state vertical profiles of the updraft vertical velocity, the rain flux within the updraft, and the rain flux that is falling into the environment. The second step involves the determination of the downdraft properties given the available rain flux and other properties of the updraft, such as its tilt.

## 4.1 Updraft Properties and Rain Flux

The CA downdraft scheme determines vertical profiles of the rain flux within the updraft and the rain flux available for the downdrafts by finding the stationary solution of the coupled rain-water budget and the vertical momentum equations for the updraft.

The stationary rain-water budget equation is written as (see Cheng 1989 for details)

$$\frac{\partial}{\partial z}\left[\frac{\eta^u}{w^u}\left(w^u - V_t^u \cos^2\theta\right)\right] + \frac{2f_2}{\pi a}\frac{\eta^u}{w^u} q_r^u V_t^u \sin\theta = \mathcal{R}, \tag{36}$$

where $w^u$ is the vertical velocity, $\theta$ is the updraft's tilting angle measured from the vertical, $a$ is an estimate of the average updraft radius, $q_r^u$ is the specific mass of rain water, and $V_t^u$ is the average terminal velocity of the rain drops in the updraft. The first and second terms on the l.h.s. of this equation represent the vertical convergence of in-cloud rain flux and the outgoing rain flux per unit height from the side of the updraft per unit cloud-base mass flux. The term on the r.h.s. is the rate of rain water generation per unit cloud-base mass flux per unit height, as given by (32).

The stationary vertical momentum equation for the updraft is written as

$$\frac{\partial}{\partial z}\left(\eta^u w^u\right)^2 = 2(\eta^u)^2 \frac{B^u - g q_r^u}{f_1(1+\gamma^*)}, \tag{37}$$

where $\gamma^* = 0.5$ is the virtual mass coefficient [3] (Simpson and Wiggert, 1969; Cheng, 1989). The term on the l.h.s. of (37) is the vertical flux divergence of the updraft

[3]The virtual mass coefficient $\gamma^*$ was introduced by Simpson and Wiggert (1969) to include the effect of acceleration of surrounding fluid.

vertical momentum, while the r.h.s. represents the vertical momentum generation by buoyancy.

The parameters $f_1$ and $f_2$ in (37) and (36) are an attempt to account for the horizontal structure of updrafts. Following Cheng (1989), we have chosen $f_1 = 2.0$ and $f_2 = 1.5$. In CA97a and CA97b, $f_1$ and $f_2$ were set to unity. The terminal velocity $V_t^u$ of the rain drops in the updraft is assumed to be given by the empirical formula:

$$V_t^u = 36.34\,(10^{-3}\rho^u q_r^u)^{0.1364}\,(\rho^u/\rho_o)^{-0.5}(\text{m s}^{-1}), \tag{38}$$

where $\rho^u$ is the updraft air density [4] and $\rho_o$ is a reference air density taken as 1.2 kg m$^{-3}$.

For a given tilting angle $\theta$, and using $V_t^u$ from (38) and $\mathcal{R}$ from (32), the discrete versions of (36) and (37) can be solved iteratively following the method described in CA97a and CA97b. CA found two types of solutions for these equations: solutions for small tilting angle, which are unstable, and solutions for large tilting angle, which are stable. They showed that the solutions for large tilting angle do not show much dependence on tilting angle $\theta$. They also pointed out that in the large tilting angle range the precise choice of $\theta$ is not very important, since the outgoing rain flux, which drives the downdraft, is more or less independent of $\theta$. In their implementation, CA chose the smallest value of $\theta$ in this stable range, after solving the above equations for a number of tilting angles.

During our experimentation with these equations, we also found that the vertical distribution of updraft rain water, the vertical velocity, and the rain flux available for the downdraft are not too sensitive to the tilting angle. Therefore, for the sake of computational economy, we prescribe a sufficiently large tilting angle (so that the solution, if it exists, belongs to the stable range at least most of the time) for each cloud type and solve (36) and (37) once for each sounding and each cloud type. If the solution exists, we invoke the downdraft; otherwise, we assume that there is no downdraft associated with that cloud type. With this approach it is possible that

[4] In our calculations, we have used the environmental air density instead of the updraft air density in (38). Since the density of the updraft air is slightly smaller than that of the environment, this approximation would decrease the terminal velocity by a few percent. Considering that (38) is empirical this assumption is not too extreme.

we may miss some downdraft solutions for some cloud types. However, we make this compromise to avoid the otherwise prohibitively expensive computations involved in following CA's approach. At present $\theta$ is prescribed as a function of the pressure at the detrainment level, varying between a value of 25° for clouds detraining at 100 hPa and 15° for those detraining at 500 hPa. The updraft radius $a$ is taken as $0.2/\lambda$ subject to an upper limit that again depends on the detrainment level. The upper limit of the radius is taken to vary between as 2 km for clouds detraining at 100 hPa and 0.25 km for those detraining at 500 hPa.

## 4.2 The Downdraft Model

Again, we follow the downdraft model of CA. For convenience, we will repeat the necessary equations. In these equations, as in CA97a and CA97b, we assume that $z$ increases downward and that mass flux and vertical velocity are positive downward. Equations governing the conservation of mass, moist static energy, and moisture in the downdraft can be written as (superscript "$d$" denotes downdraft quantities)

$$\frac{d\eta^d}{dz} = \epsilon - \delta, \tag{39a}$$

$$\frac{d\eta^d h^d}{dz} = \epsilon h - \delta h^d, \tag{39b}$$

$$\frac{d\eta^d q^d}{dz} = \epsilon q - \delta q^d + E_r, \tag{39c}$$

where $\eta^d$ is the downdraft mass flux normalized by the cloud-base mass flux of the updraft, $M_B$; $\epsilon$, and $\delta$ are the normalized entrainment into and detrainment from the downdraft; $h^d$ and $q^d$ are the moist static energy and specific humidity of the downdraft air; and $E_r$ is moisture source due to evaporation of falling rain, taken as

$$E_r = \sigma \frac{(1 - q^d/q^{*d})\, C\, (10^{-3}\rho^d q_r^d)^{0.525}}{5.4 \times 10^5 + 2.55 \times 10^6/(pq^{*d})}, \tag{40}$$

where $\sigma$ is the fractional horizontal area covered by the downdraft per unit cloud-base mass flux of the updraft; $q^{*d}$, $q_r^d$, and $\rho^d$ are the downdraft saturation specific humidity, specific mass of rain water, and air density, respectively; $p$ is the pressure

in units of hPa; and $C$ is a nondimensional ventilation coefficient, given by

$$C = 1.6 + 124.9\,(10^{-3}\rho^d q_r)^{0.2046}. \tag{41}$$

The vertical momentum equation, the rain-water budget equation, and the equation governing the vertical variation of $\sigma$ for the downdraft as used by CA are:

$$\frac{d\eta^d w^d}{dz} = -\frac{\eta^d}{w^d}\frac{B^d - g q_r^d}{f_5(1+\gamma^*)} - \delta w^d, \tag{42}$$

$$\frac{dP^d}{dz} = \mathcal{R}_A - E_r, \tag{43}$$

and

$$\frac{\partial \sigma}{\partial z} = \frac{V_t^d}{w^d + V_t^d}\left(\frac{2}{\rho^u \pi a}\frac{\eta^u}{w^u}\sin\theta\right) - \frac{\sigma}{\rho^d}\frac{1}{w^d + V_t^d}\frac{\partial \rho^d w^d}{\partial z} - \sigma\frac{E_r}{P^d}, \tag{44}$$

where $P^d$ is the rain-water flux in the downdraft given by,

$$P^d = \rho^d \sigma q_r^d\,(w^d + V_t^d), \tag{45}$$

and $\mathcal{R}_A$ is the normalized updraft rain water flux per unit height available for the downdraft, given by

$$\mathcal{R}_A = \left(\frac{2}{\pi a}\frac{\eta^u}{w^u} q_r^u V_t^u \sin\theta\right). \tag{46}$$

The downdraft air density at the level of downdraft origin is assumed to be identical to the environmental density. For all other levels, it is determined as a part of the solution to the set of downdraft equations given above. The terminal velocity, $V_t^d$, of falling precipitation in the downdraft is determined by the empirical formula (38) with $q_r^d$ and $\rho^d$ in place of $q_r^u$ and $\rho^u$. In the first term of the r.h.s. of (44) the updraft density $\rho^u$ is approximated by the environmental air density. The parameter $f_5$ in (42) relates to the horizontal structure of the downdraft; following Cheng (1989), we have chosen $f_5 = 2.5$. A detailed description of the iterative solution of the discrete forms of the above set of equations is available in CA97b. We have basically followed their procedure, but with some deviations, which are discussed along with the discrete formulation.

# 5 Modification of the Environment

## 5.1 Cumulus Effects on the Large-scale Budget

As in MS, we divide the continuous spectrum of clouds into subensembles of finite $\Delta\lambda_i$. Thus, the rate of change of environmental temperature, specific humidity, specific mass of liquid water, and specific mass of ice water due to the $i^{th}$ cloud ensemble with entrainment parameter between $\lambda_i$ and $\lambda_i + \Delta\lambda_i$ can be written as

$$\left(\frac{\partial T}{\partial t}\right)_c = \frac{M_B(\lambda_i)\Delta\lambda_i}{c_p}\,\Gamma_s, \tag{47}$$

$$\left(\frac{\partial q}{\partial t}\right)_c = \frac{M_B(\lambda_i)\Delta\lambda_i}{L_c}\,[\Gamma_h - \Gamma_s + L_f\Gamma_I], \tag{48}$$

$$\left(\frac{\partial q^L}{\partial t}\right)_c = \frac{M_B(\lambda_i)\Delta\lambda_i}{c_p}\,\Gamma_L, \tag{49}$$

and

$$\left(\frac{\partial q^I}{\partial t}\right)_c = \frac{M_B(\lambda_i)\Delta\lambda_i}{c_p}\,\Gamma_I, \tag{50}$$

where $\Gamma_s$, $\Gamma_h$, $\Gamma_L$ and $\Gamma_I$ are the convection induced rates of change of environmental dry static energy $s$, moist static energy $h$, specific mass of liquid water $q^L$, and specific mass of ice water $q^I$ per unit cloud-base mass flux $M_B(\lambda_i)\Delta\lambda_i$.

In evaluating $\Gamma_s$ and $\Gamma_h$, we include contributions from both the updraft and downdraft associated with each subensemble. Thus,

$$\Gamma_s = g\left[\delta^u(s^u - s) - \eta^u\frac{\partial s}{\partial p} + \frac{\partial\{\eta^d(s^d - s)\}}{\partial p}\right] \tag{51}$$

and

$$\Gamma_h = g\left[\delta^u(h^u - h) - \eta^u\frac{\partial h}{\partial p} + \frac{\partial\{\eta^d(h^d - h)\}}{\partial p}\right], \tag{52}$$

where $\delta^u$ is the detrainment per unit pressure interval in the updraft. In our current formulation, we allow detrainment of condensate from the updraft only at the cloud top. In evaluating $\Gamma_L$ and $\Gamma_I$, we include only contributions from the updraft:

$$\Gamma_L = g\left[\delta^u(q^{uL} - q^L) - \eta^u \frac{\partial q^L}{\partial p}\right] \tag{53}$$

and

$$\Gamma_I = g\left[\delta^u(q^{uI} - q^I) - \eta^u \frac{\partial q^I}{\partial p}\right]. \tag{54}$$

If the environment does not contain liquid water or ice, then (53) and (54) have a contribution only from detrainment. Discrete forms of these equations are given in the next section.

It should be noted that in (51)-(54) we do not allow for phase changes of cloud condensate during detrainment. Depending on the application and on the parameterization of microphysical and precipitation processes in other parts of the model, one may wish to modify this assumption. In the present application, we are assuming that the detrained condensate is available as a source term for the prediction of condensate in the environment.

## 5.2 The Mass-flux Kernel and Cloud Base Mass Flux

The mass-flux kernel is defined as the rate of change of cloud work function per unit cloud-base mass flux. In MS the mass-flux kernel was determined analytically by differentiating the expression for the cloud work function. However, it is difficult to do so with the cloud work function as defined in (30). Therefore, we calculate the mass-flux kernel numerically by following the approach used in the standard implementation of AS as in Lord et al. (1982). In this approach we first calculate the cloud work function of a subensemble; we then use a small "test" cloud-base mass flux and modify the sounding using (47) and (48). Using this modified sounding, we recalculate the cloud work function. The mass-flux kernel $\mathcal{K}_i$ is then estimated as the change in the cloud work function divided by the test mass flux.

Once the mass-flux kernel is known, we can compute the cloud-base mass flux nec-

essary to completely balance the large-scale effects on the cloud work function (see MS and Lord et al., 1982, for further details). The final adjustment of the large-scale environment is then made using a fraction $\alpha_{\lambda_i}$ of the mass flux needed to fully adjust a single cloud type (see MS). Thus, both the updraft and downdraft associated with a subensemble modify the environment when that subensemble is invoked and thus influence both updraft and downdraft properties of all subensembles invoked subsequently.

## 5.3 Evaporation of Falling Precipitation

The precipitation generated in the updraft eventually falls into the environment or the subcloud layer. Such falling precipitation in an unsaturated environment undergoes evaporation, often producing downdrafts. In the original RAS, evaporation of falling precipitation was not included. Moorthi (1999) included a simple scheme based on the formulation of Sud and Molod (1988) in the original RAS. In the version of RAS presented here, evaporation in the environment and the associated downdraft are determined using the CA approach. However, we do encounter situations in which a downdraft does not form. Also, we may not perform downdraft calculations for shallow cloud types to save computer time. Furthermore, we allow the option of starting the downdraft from a level below the top of the updraft. For all of these situations, we compute the evaporation of falling precipitation following the Sud and Molod (1988) approach as described in Moorthi (1999). For completeness, we provide some details of this approach in Appendix B.

When no downdraft exists or when there is no solution for the rain flux equation (36), we assume that all rain falls into the environment at the level where it is generated, as in the original AS. This rain profile is used in the evaporation calculation. If a solution to the rain flux equation (36) exists, but no downdraft solution exists, then the rain flux profile is used as the rain available for evaporation. If the downdraft calculation is done from a level below the updraft top, then any rain flux above that level is also available for evaporation outside of downdraft. Also, if the downdraft stops before reaching the ground due to loss of buoyancy, then the rain falling through

the bottom of the downdraft undergoes evaporation. Rain falling from the bottom of the updraft may also contribute to evaporation in the subcloud layer. Finally, there can be situations when we start the downdraft calculation from a layer (*e.g.* cloud top), but downdraft does not start (*i.e.* no solution to downdraft equations) in this layer. For these situations, we simply let the rain flux drop to the layer below until the downdraft starting level is reached.

# 6 Vertically Discrete Formulation

We now consider the vertically discrete system. In order to resolve the planetary boundary layer, most modern models have many layers in the lower troposphere. Therefore, in our present discrete formulation, we allow for more than one layer below the cloud base. Thus, we divide the vertical domain into $K + M - 1$ layers and index the variables vertically from top to bottom. Layer 1 represents the top layer of the atmosphere, while layer $K$ represents the first layer in the subcloud layer just below the cloud base and $M$ is the total number of subcloud layers ($M \geq 1$). Any layer $k$ is bounded by edge levels $k - \frac{1}{2}$ and $k + \frac{1}{2}$. The environmental temperature $T$, specific humidity $q$, and any condensate are assumed to be defined at the layers. A schematic of the vertical grid is shown in figure 2 with two subcloud layers and a tilted updraft with an associated downdraft.

## 6.1 The Hydrostatic Equation

Letting $\hat{\phi}_{k+\frac{1}{2}}$ be the geopotential for edge $k + \frac{1}{2}$, (3) is finite-differenced as

$$\hat{\phi}_{k-\frac{1}{2}} = \hat{\phi}_{k+\frac{1}{2}} + \theta_{\mathrm{v}k} \left(\hat{\Pi}_{k+\frac{1}{2}} - \hat{\Pi}_{k-\frac{1}{2}}\right), \tag{55}$$

where $\theta_{\mathrm{v}k} = c_p \frac{T_{\mathrm{v}k}}{\Pi_k}$

$$\Pi_k = \frac{1}{(1+\kappa)} \frac{\hat{\Pi}_{k+\frac{1}{2}} \hat{p}_{k+\frac{1}{2}} - \hat{\Pi}_{k-\frac{1}{2}} \hat{p}_{k-\frac{1}{2}}}{(\hat{p}_{k+\frac{1}{2}} - \hat{p}_{k-\frac{1}{2}})}, \tag{56}$$

and $\hat{\Pi}_{k+1/2}$ is evaluated at the edge pressure $\hat{p}_{k+\frac{1}{2}}$.

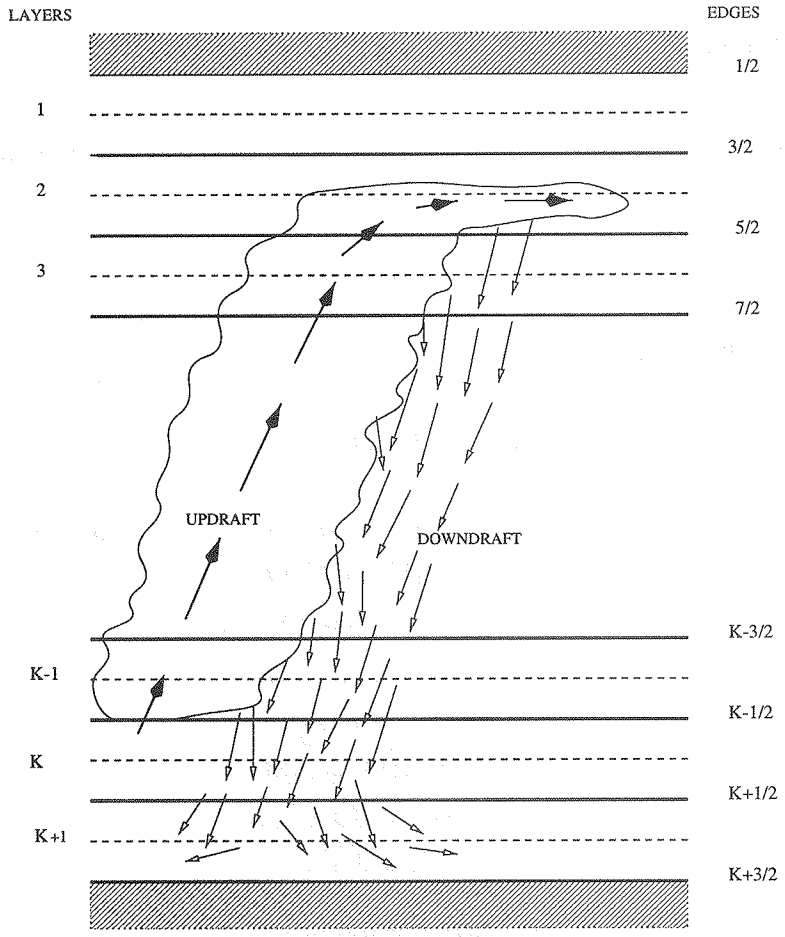


Figure 2: The vertical grid

Layer values of the geopotential are defined as

$$\phi_k = \hat{\phi}_{k+\frac{1}{2}} + \theta_{vk}\,(\hat{\Pi}_{k+\frac{1}{2}} - \Pi_k). \tag{57}$$

From (55) and (57), we can obtain the upper and lower half-layer thicknesses

$$\hat{\phi}_{k-\frac{1}{2}} - \phi_k = \theta_{vk}\,(\Pi_k - \hat{\Pi}_{k-\frac{1}{2}}), \tag{58a}$$

and

$$\phi_k - \hat{\phi}_{k+\frac{1}{2}} = \theta_{vk}\,(\hat{\Pi}_{k+\frac{1}{2}} - \Pi_k). \tag{58b}$$

We define the layer pressure, $p_k$, as

$$p_k = \frac{1}{2}(\hat{p}_{k-\frac{1}{2}} + \hat{p}_{k+\frac{1}{2}}). \tag{59}$$

## 6.2 The Entrainment Relation

Below the updraft top, the normalized mass flux $\eta^u$ is defined at the layer edges and is assumed to have the form

$$\eta^u_{k-\frac{1}{2}} = 1 + \lambda\zeta_{k-\frac{1}{2}} + \lambda^2\xi_{k-\frac{1}{2}} \tag{60}$$

for $k = i+1, i+2, \ldots, K-1$, where

$$\zeta_{k-\frac{1}{2}} = (z_{k-\frac{1}{2}} - z_B) \tag{61a}$$

and

$$\xi_{k-1/2} = \frac{1}{2}(z_{k-\frac{1}{2}} - z_B)^2, \tag{61b}$$

where, $z_B$ is the height of the top of the subcloud layer. At the updraft top (denoted by integer level $i$), we define the normalized mass flux as

$$\eta^u_i = 1 + \lambda\zeta_i + \lambda^2\xi_i, \tag{62}$$

where

$$\zeta_i = (z_i - z_B) \tag{63a}$$

and

$$\xi_i = \frac{1}{2}(z_i - z_B)^2. \tag{63b}$$

Then,

$$\eta^u_{k-\frac{1}{2}} = \eta^u_{k+\frac{1}{2}} + \lambda(\zeta_{k-\frac{1}{2}} - \zeta_{k+\frac{1}{2}}) + \lambda^2(\xi_{k-\frac{1}{2}} - \xi_{k+\frac{1}{2}}) \tag{64}$$

and

$$\eta^u_i = \eta^u_{i+\frac{1}{2}} + \lambda(\zeta_i - \zeta_{i+\frac{1}{2}}) + \lambda^2(\xi_i - \xi_{i+\frac{1}{2}}). \tag{65}$$

## 6.3 The Condensate Budget and the Entrainment Parameter

The discrete form of the condensate budget (33) can be written as

$$\eta^u_{k-\frac{1}{2}} q^{uC}_{k-\frac{1}{2}} = \eta^u_{k+\frac{1}{2}} q^{uC}_{k+\frac{1}{2}} + \eta^u_{k+\frac{1}{2}} q^u_{k+\frac{1}{2}} - \eta^u_{k-\frac{1}{2}} q^u_{k-\frac{1}{2}} + (\eta^u_{k-\frac{1}{2}} - \eta^u_{k+\frac{1}{2}}) q^T_k - \mathcal{R}_k, \tag{66}$$

for all $k = i+1, \ldots, K-1$, where $\mathcal{R}_k$ is the rate conversion of condensate to rain. When $k = K-1$ in (66), $q^u_{K-\frac{1}{2}} = q_B$, the specific humidity of the subcloud layer air entering the updraft. [5] Similarly, discretizing (33) over the lower half of the top layer of the updraft, between levels $i$ and $i+\frac{1}{2}$, we can write

$$\eta^u_i q^{uC}_i = \eta^u_{i+1/2} q^{uC}_{i+\frac{1}{2}} + \eta^u_{i+\frac{1}{2}} q^u_{i+\frac{1}{2}} - \eta^u_i q^u_i + (\eta^u_i - \eta^u_{i+\frac{1}{2}}) q^T_i - \mathcal{R}_i, \tag{67}$$

where $\mathcal{R}_i$ is the rate conversion of condensate to rain in the top layer. We choose the following form for $\mathcal{R}_k$:

$$\mathcal{R}_k = c_o \left[ \tilde{a}_k \eta^u_{k-\frac{1}{2}} q^{uC}_{k-\frac{1}{2}} + \tilde{b}_k \eta^u_{k+\frac{1}{2}} q^{uC}_{k+\frac{1}{2}} \right], \tag{68}$$

for all $k = i+1, \ldots, K-1$, where $c_o$ is the auto conversion coefficient, $\tilde{a}_k = (p_k - \hat{p}_{k-\frac{1}{2}})/(\hat{p}_{k+\frac{1}{2}} - \hat{p}_{k-\frac{1}{2}})$ and $\tilde{a}_k + \tilde{b}_k = 1$. The term inside the square brackets is an approximation to the term $\eta^u_k q^{uC}_k$ used in Lord's formulation. At the detrainment level $i$ we use

$$\mathcal{R}_i = c_o \left[ \tilde{a}_i \eta^u_i q^{uC}_i + \tilde{b}_i \eta^u_{i+\frac{1}{2}} q^{uC}_{i+\frac{1}{2}} \right]. \tag{69}$$

We assume that no cloud condensate enters the updraft through the bottom, *i.e.*, $q^{uC}_{K-\frac{1}{2}} = 0$. Substituting (68) and (69) in (66) and (67), we can write the discrete condensate budget as

$$a_k \eta^u_{k-\frac{1}{2}} q^{uC}_{k-\frac{1}{2}} = b_k \eta^u_{k+\frac{1}{2}} q^{uC}_{k+\frac{1}{2}} + \eta^u_{k+\frac{1}{2}} q^u_{k+\frac{1}{2}} - \eta^u_{k-\frac{1}{2}} q^u_{k-\frac{1}{2}} + (\eta^u_{k-\frac{1}{2}} - \eta^u_{k+\frac{1}{2}}) q^T_k, \tag{70}$$

where

$$a_k = 1 + c_o \tilde{a}_k (z_{k-\frac{1}{2}} - z_{k+\frac{1}{2}}) \tag{71a}$$

and

$$b_k = 1 - c_o \tilde{b}_k (z_{k-\frac{1}{2}} - z_{k+\frac{1}{2}}) \tag{71b}$$

for all $k = i+1, \ldots K-1$, and

$$a_i \eta^u_i q^{uC}_i = b_i \eta^u_{i+\frac{1}{2}} q^{uC}_{i+\frac{1}{2}} + \eta^u_{i+\frac{1}{2}} q^u_{i+\frac{1}{2}} - \eta^u_i q^u_i + (\eta^u_i - \eta^u_{i+\frac{1}{2}}) q^T_i, \tag{72}$$

where

$$a_i = 1 + c_o \tilde{a}_i (z_i - z_{i+\frac{1}{2}}) \tag{73a}$$

[5] When there is more than one model layer in the subcloud layer, we need to make some assumption regarding the property of the air entering the updraft through the cloud base. Presently, we are using a mass-weighted mean of the subcloud layer values for both the specific humidity and the moist static energy entering the updraft.

and

$$b_i = 1 - c_o \tilde{b}_k (z_i - z_{i+\frac{1}{2}}) \tag{73b}$$

at the updraft top. It should be remarked that the above treatment of the moisture budget within a updraft layer is very simplistic compared to the standard implementation of Arakawa-Schubert as described in CA97b. Nevertheless, it is an improvement over the precipitation formulation in the original RAS, while still retaining the capability to solve for the entrainment parameter in an economical way (by avoiding the iteration needed in the standard implementation).

The discrete form of the updraft moist static energy budget (13) can be written as

$$\eta^u_{k-\frac{1}{2}} h^u_{k-\frac{1}{2}} = h_B + \sum_{K-1}^{k} (\eta^u_{j-\frac{1}{2}} - \eta^u_{j+\frac{1}{2}}) h_j, \tag{74}$$

for all $k = i+1, \ldots, K-1$, and

$$\eta^u_i h^u_i = \eta^u_{i+\frac{1}{2}} h^u_{i+\frac{1}{2}} + (\eta^u_i - \eta^u_{i+\frac{1}{2}}) h_i, \tag{75}$$

at the updraft top. Here, $h_B$ is the subcloud layer's moist static energy, which is entering the updraft from below. Using (74), (25), (8), (60), and (62) in (70) and (72), and after simplification (see the Appendix A for details), we obtain the following quadratic form for the condensate at the updraft detrainment level:

$$\eta^u_i q^{uC}_i = \lambda^2 \tilde{H} + \lambda \tilde{G} + \tilde{F}. \tag{76}$$

Using (76) in the non-buoyancy condition (35) applied at the cloud top and after further manipulations (see the Appendix A), we can obtain a quadratic equation in the entrainment parameter $\lambda$ whose coefficients depend only on environmental quantities. Once $\lambda$ is obtained from this equation, we can obtain the normalized mass flux $\eta^u$ from (60) and (62), and the cloud moist static energy $h^u$ from (74) and (75). Then using (25), we can obtain $q^u$, the in-cloud specific humidity, at the updraft top as well as at the layer edges. Subsequently, we can obtain the vertical profiles of the total condensate $q^{uC}$, cloud suspended liquid water $q^{uL}$ and ice $q^{uI}$. Then the rain $\mathcal{R}_k$ produced at level $k$ can be obtained from (68) and (69).

## 6.4 Calculation of Downdraft Properties

As mentioned before, we have followed the procedure of CA in determining the downdraft properties, with some minor modifications. We have coded the solution procedure such that we can start the downdraft from any level at or below the level of detrainment of the updraft. Discrete forms of the set of downdraft equations (39)-(45) are solved iteratively, one layer at a time, starting from the top of the downdraft. All downdraft properties are calculated at the half-integer levels.

The solution of the discrete form of (44) for the fractional area covered by the downdraft, $\sigma$, requires a boundary condition at the top of the downdraft. We simply specify a $\sigma$ at the top by considering only the tilting term in (44). Thus, if the downdraft calculation starts from the updraft detrainment level $i$, then we assume:

$$\sigma_i = \left(\frac{2}{\rho^u \pi a}\frac{\eta^u}{w^u} sin\theta\right)_i (z_i - z_{i-\frac{1}{2}}). \tag{77}$$

If the downdraft calculation starts from a level $k+\frac{1}{2}$ below the level $i$, then we take:

$$\sigma_{k+\frac{1}{2}} = \left(\frac{2}{\rho^u \pi a}\frac{\eta^u}{w^u} sin\theta\right)_{k-\frac{1}{2}} (z_{k-\frac{1}{2}} - z_k) + \left(\frac{2}{\rho^u \pi a}\frac{\eta^u}{w^u} sin\theta\right)_{k-\frac{1}{2}} (z_k - z_{k+\frac{1}{2}}). \tag{78}$$

For levels below the downdraft starting level, we solve (44) by adopting the following discretization:

$$\begin{aligned}\sigma_{k+\frac{1}{2}} = \sigma_{k-\frac{1}{2}} + \Bigg[ & \left\{\frac{V_t^d}{w^d + V_t^d}\left(\frac{2}{\rho^u \pi a}\frac{\eta^u}{w^u} sin\theta\right)\right\}_{k-\frac{1}{2}} (z_k - z_{k-\frac{1}{2}}) \\ & + \left\{\frac{V_t^d}{w^d + V_t^d}\left(\frac{2}{\rho^u \pi a}\frac{\eta^u}{w^u} sin\theta\right)\right\}_{k+\frac{1}{2}} (z_{k+\frac{1}{2}} - z_k) \\ & - \frac{2}{\left\{\rho^d q_r^d (w^d + V_t^d)\right\}_{k-\frac{1}{2}} + \left\{\rho^d q_r^d (w^d + V_t^d)\right\}_{k+\frac{1}{2}}} (E_r \Delta z)_k \Bigg] \\ & \times \left[1 + \frac{1}{\rho^d_{k+\frac{1}{2}}} \frac{1}{(w^d + V_t^d)_{k+\frac{1}{2}}} \left((\rho^d w^d)_{k+\frac{1}{2}} - (\rho^d w^d)_{k-\frac{1}{2}}\right)\right]^{-1}. \end{aligned} \tag{79}$$

This discretization is simpler than the one used by CA. In the CA implementation, they sub-divide each model layer into several layers of smaller thickness for the down-

draft calculation. In our implementation, we perform the downdraft calculation on the original grid assuming that the vertical resolution is reasonably fine. If the vertical resolution is too coarse, the downdraft calculation may not converge. The mass flux at the downdraft starting level is taken as zero. If the iteration does not converge for the next lower level, then it is assumed that there is no downdraft in that layer and the rain flux is simply added to the next layer without evaporation. The procedure is repeated for all layers below. Care is needed to properly treat the situation when the downdraft loses its negative buoyancy before reaching the bottom layer of the model. Unlike CA, we allow the downdraft to penetrate the layers below the cloud base by explicitly calculating the downdraft properties in all subcloud layers including the layer next to the bottom surface. In applying (79) to levels below the cloud base, we use the fact that there is zero contribution from the tilting term. The downdraft airmass, after impinging on the bottom boundary, is assumed to modify the subcloud layer properties.

We implement this updraft/downdraft scheme one cloud-type at a time. As discussed before, the downdraft directly modifies the mass flux kernel of this cloud-type. As in the original RAS, interaction between different cloud-types is through subsequent invocation of other cloud types.

## 6.5 Cumulus Effects on the Large-scale Environment

The discrete forms of the budgets of the dry and moist static energies in the environment are written in the form

$$\left(\frac{\partial s_k}{\partial t}\right)_c = M_B \Gamma_s(k), \tag{80}$$

$$\left(\frac{\partial h_k}{\partial t}\right)_c = M_B \Gamma_h(k), \tag{81}$$

where $\Gamma_s(k)$ and $\Gamma_h(k)$ are the rate of change of dry and moist static energies of the environment per unit cloud-base mass flux. In discrete form, they are given by

$$\begin{aligned} \Gamma_s(k) &= \frac{g}{\Delta p_k}\left[\eta^u_{k-\frac{1}{2}}(s_{k-\frac{1}{2}} - s_k) + \eta^u_{k+\frac{1}{2}}(s_k - s_{k+\frac{1}{2}}) + \delta_{i,k}\eta^u_i(s^u_i - s_i)\right. \\ &+ \left.\eta^d_{k-\frac{1}{2}}(s^d_{k-\frac{1}{2}} - s_{k-\frac{1}{2}}) - \eta^d_{k+\frac{1}{2}}(s^d_{k+\frac{1}{2}} - s_{k+\frac{1}{2}}) - L_c(E_r\Delta z)_k\right], \end{aligned} \tag{82}$$

and

$$\begin{aligned}\Gamma_h(k) &= \frac{g}{\Delta p_k}\Big[\eta^u_{k-\frac{1}{2}}(h_{k-\frac{1}{2}}-h_k)+\eta^u_{k+\frac{1}{2}}(h_k-h_{k+\frac{1}{2}})+\delta_{i,k}\eta^u_i(h^u_i-h_i)\\ &+ \eta^d_{k-\frac{1}{2}}(h^d_{k-\frac{1}{2}}-h_{k-\frac{1}{2}})-\eta^d_{k+\frac{1}{2}}(h^d_{k+\frac{1}{2}}-h_{k+\frac{1}{2}})\Big], \qquad (83)\end{aligned}$$

for $k = i, i+1\ldots., K-1$, and

$$\begin{aligned}\Gamma_s(k) &= \frac{g}{\Delta p_k}\Big[r_k(s_{K-\frac{1}{2}}-s_B+\eta^d_{K+M-\frac{1}{2}}\{s^d_{K+M-\frac{1}{2}}-s_{K+M-\frac{1}{2}}\})\\ &+ \eta^d_{k-\frac{1}{2}}(s^d_{k-\frac{1}{2}}-s_{k-\frac{1}{2}})-\eta^d_{k+\frac{1}{2}}(s^d_{k+\frac{1}{2}}-s_{k+\frac{1}{2}})-L_c(E_r\Delta z)_k\Big], \qquad (84)\end{aligned}$$

and

$$\begin{aligned}\Gamma_h(k) &= \frac{g}{\Delta p_k}\Big[r_k(h_{K-\frac{1}{2}}-h_B+\eta^d_{K+M-\frac{1}{2}}\{h^d_{K+M-\frac{1}{2}}-h_{K+M-\frac{1}{2}}\})\\ &+ \eta^d_{k-\frac{1}{2}}(h^d_{k-\frac{1}{2}}-h_{k-\frac{1}{2}})-\eta^d_{k+\frac{1}{2}}(h^d_{k+\frac{1}{2}}-h_{k+\frac{1}{2}})\Big], \qquad (85)\end{aligned}$$

for $k = K, K+1\ldots., K+M-1$, where

$$r_k = \frac{\Delta p_k}{p_{K+M-\frac{1}{2}}-p_{K-\frac{1}{2}}}. \qquad (86)$$

Here $\eta^d_{k-\frac{1}{2}}$ is the downdraft mass flux at level $k-\frac{1}{2}$ per unit cloud-base updraft mass flux $M_B$, $s^d_{k-\frac{1}{2}}$ and $h^d_{k-\frac{1}{2}}$ are the dry and moist static energies in the downdraft, $(E_r\Delta z)_k$ is the normalized rain evaporation rate in layer $k$ in the downdraft, and $\delta_{i,k}$ is the Kronecker delta. The terms with $\delta_{i,k}$ represent detrainment effects, which occur only in the cloud top layer. If we allow for detrainment from other layers, then these equations need to be modified. Also, note that in (82) and (83) we have used $\eta_{i-\frac{1}{2}} = 0$. Below the cloud-base, the subcloud layer is treated as a single layer as far as the updraft effects are concerned (see (84) and (85)). Thus all layers in the subcloud layer experience equal changes due to updraft effects. The downdraft effects are computed individually for all layers in the subcloud layer. In (84) and (85), $s_B$ and $h_B$ are the subcloud layer values of dry and moist static energies entering the updraft. We have also assumed that the downdraft airmass, after impinging on the bottom boundary, mixes within the subcloud layer and the corresponding terms are also included in (84) and (85).

Similar equations can be written for the rate of change of environmental liquid water and ice:

$$\Gamma_L(k) = \frac{g}{\Delta p_k}\left[\eta^u_{k-\frac{1}{2}}(q^L_{k-\frac{1}{2}} - q^L_k) + \eta^u_{k+\frac{1}{2}}(q^L_k - q^L_{k+\frac{1}{2}}) + \delta^k_i \eta^u_i (q^{uL}_i - q^L_i)\right], \quad (87)$$

and

$$\Gamma_I(k) = \frac{g}{\Delta p_k}\left[\eta^u_{k-\frac{1}{2}}(q^I_{k-\frac{1}{2}} - q^I_k) + \eta^u_{k+\frac{1}{2}}(q^I_k - q^I_{k+\frac{1}{2}}) + \delta^k_i \eta^u_i (q^{uI}_i - q^I_i)\right], \quad (88)$$

for $k = i, i+1, \ldots, K-1$, where we have ignored the downdraft effects. [6]

From (82), (83) and (88), we can obtain the rate of change of temperature and moisture due to cumulus effects as

$$\left(\frac{\partial T_k}{\partial t}\right)_c = \frac{M_B}{c_p}\Gamma_s(k), \quad (89)$$

and

$$\left(\frac{\partial q_k}{\partial t}\right)_c = \frac{M_B}{L_c}\left[\Gamma_h(k) - \Gamma_s(k) + L_f\Gamma_I(k)\right]. \quad (90)$$

## 6.6 The Cloud Work Function, Mass-flux Kernel and Cloud Base Mass Flux

Once we have determined the entrainment parameter, the normalized mass flux, vertical profiles of cloud moist static energy, and total water and its components, we can calculate the cloud work function. We discretize (31) as follows:

$$\begin{aligned}\mathcal{A}_i = \sum_{K-1}^{i+1} \frac{1}{\tilde{L}_k}\Big[&\left(h^u_{k-\frac{1}{2}} + L_f q^{uI}_{k-\frac{1}{2}} - h^{**}_k - \tilde{L}_k(q^{uC}_{k-\frac{1}{2}} - q^L_k - q^I_k)\right)\eta^u_{k-\frac{1}{2}}(\phi_{k-\frac{1}{2}} - \phi_k) \\ &+ \left(h^u_{k+\frac{1}{2}} + L_f q^{uI}_{k+\frac{1}{2}} - h^{**}_k - \tilde{L}_k(q^{uC}_{k+\frac{1}{2}} - q^L_k - q^I_k)\right)\eta^u_{k+\frac{1}{2}}(\phi_k - \phi_{k+\frac{1}{2}})\Big] \\ &+ \frac{1}{2\tilde{L}_i}\left[h^u_{i+\frac{1}{2}} + L_f q^{uI}_{i+\frac{1}{2}} - h^{**}_{i+\frac{1}{2}} - \tilde{L}_{i+\frac{1}{2}}(q^{uC}_{i+\frac{1}{2}} - q^L_{i+\frac{1}{2}} - q^I_{i+\frac{1}{2}})\right]\eta^u_{i+\frac{1}{2}}(\phi_i - \phi_{i+\frac{1}{2}}). \quad (91)\end{aligned}$$

[6] During our testing with this discretization for the liquid water and ice, we discovered that it can easily produce negative values, since the scheme is not positive definite and the condensate field can be highly discontinuous in the vertical. Because of this, in the results presented in this report, we ignore the condensate in the environment. Then (87) and (88) will have non-zero values only at the detrainment level. Neglect of environmental condensate implies that cloud-types cannot recognize the condensate in the environment detrained by the previously invoked cloud-types. We do not view this as a serious limitation.

The values of $h^{**}_{i+\frac{1}{2}}$, $\tilde{L}_{i+\frac{1}{2}}$, $q^{L}_{i+\frac{1}{2}}$, and $q^{I}_{i+\frac{1}{2}}$ in (91) are taken as averages of those at integer levels $i$ and $i+1$.

As in CA97b, we have not included downdraft effects in the calculation of the cloud work function. Justification for doing so is provided by CA97a. Following the procedure described in subsection 5.2, we calculate $\mathcal{K}_i$ numerically using (91). If $\mathcal{K}_i$ is positive, then such a cloud type cannot exist. The large-scale forcing can be computed from the cloud work function as described in MS. Once the kernel and the large-scale forcings are known, the cloud-base mass flux and the adjustments to the large-scale environment can be calculated.

# 7 Semi-Prognostic Evaluation

As demonstrated by Lord (1978, 1982), Krishnamurti et. al., (1980), Kao and Ogura (1987), and others, the semi-prognostic test is a very useful tool in the development and evaluation of a cumulus parameterization scheme. The original version of RAS was tested by MS using both the semi-prognostic and the single column prognostic approach. MS found that while the obtained cumulus heating profile was reasonable, the cumulus drying was excessive compared to the observed estimate. This result is consistent with those for the original implementation, as shown in Lord (1978). Moorthi (1999) showed that inclusion of evaporation of falling convective rain does not completely reduce the excessive drying. We have tested the new RAS described herein with the semi-prognostic approach also and the results are reported in this section.

For this purpose, we use the same GATE phase III data employed by MS. The daily mean radiation data are from Cox and Griffith (1978) and all other data are as analyzed by Thompson et al., (1979). Surface evaporation and sensible heat flux, and the turbulent fluxes in the boundary layer are estimated using the boundary layer formulation of the National Centers for the Environmental Prediction (NCEP) Medium Range Forecast (MRF) model (Hong and Pan, 1996). We use 19 layers of equal pressure depth in the vertical between the surface and the top of the atmosphere.

The lowest model layer is considered as the subcloud layer for this semi-prognostic test although the new RAS code allows for the subcloud layer to contain more than one model layer.

We have performed two sets of semi-prognostic tests. In the first set, the values of moist static energy and moisture at the subcloud layer top (level $K - \frac{1}{2}$) are assumed to be the same as the corresponding subcloud layer values, $h_B$ and $q_B$ (*i.e.* Moorthi, 1999). In this case, cumulus induced subsidence cannot directly modify the boundary layer, as in the original implementation of AS (Lord et al., 1982). In the second set, the values of the moist static energy and moisture at the top of the subcloud layer are taken as a mean of the corresponding values within the subcloud layer and the layer above. In this case, cumulus induced subsidence can directly modify the boundary layer and this may result in substantial differences. In both sets of experiments, however, the downdraft is allowed to penetrate the subcloud layer.

Figure 3a,b shows the time-averaged convective heating and moistening as a function of height obtained in the experiments in which the cumulus subsidence cannot directly modify the subcloud layer. In these figures, thick solid lines (RV1) correspond to version 1 of RAS, as currently used at NCEP, with evaporation of falling precipitation. It also includes evaporation of part of the rain at the detrainment level when the cloud top is below 400 hPa. The thin solid lines (RV2LND) are for the RAS version 2 with the linear entrainment relation and no downdraft. This version of RAS also includes evaporation of falling precipitation as used in RV1. We also allow the detrained condensate at the cloud top to partially evaporate in the environment as it falls, using a scheme similar to that used for evaporation of falling large-scale precipitation in the NCEP operational global model. The long dashed lines (RV2QND) are for RAS version 2 with the quadratic entrainment relation and no downdraft. The dotted lines (RV2QDT) are for RAS version 2 with the quadratic entrainment relation and a downdraft starting from the detrainment level. The short dashed lines (RV2QDM) are for the case when the downdraft is allowed to start from the level of minimum moist static energy. The thick dash-dot lines are an observed estimate of cumulus heating and moistening. They are obtained from the apparent heat source, $Q_1$, and moisture sink, $Q_2$ (Yanai et al., 1973), in the GATE data set, with daily mean radiation

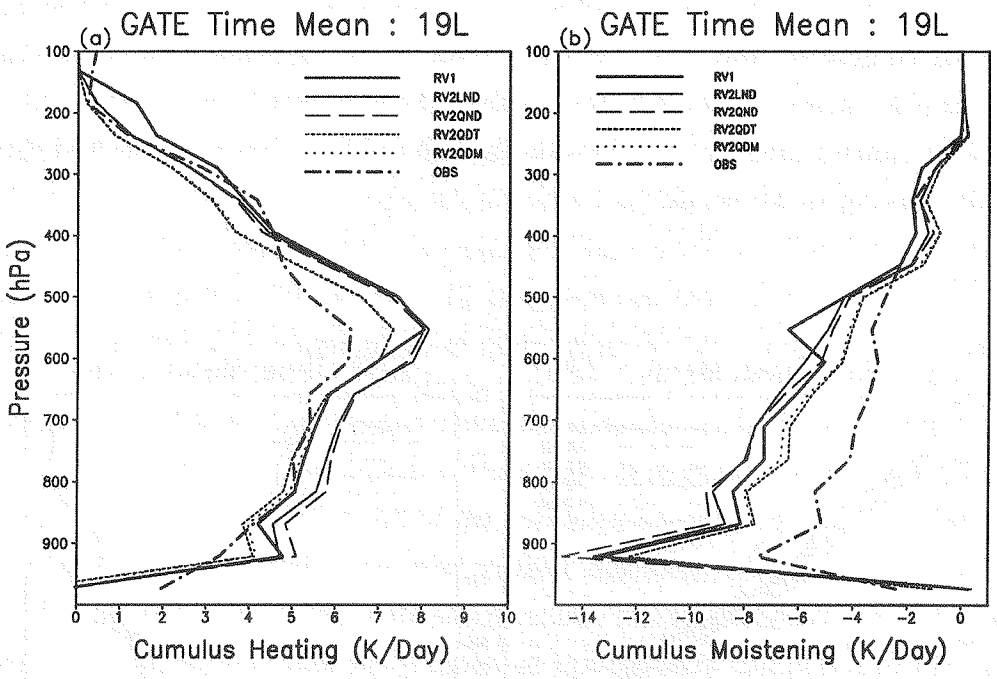


Figure 3: The time-averaged convective (a) heating (K/day) and (b) moistening (K/day) as a function of height obtained in the semi-prognostic test using the GATE Phase III data. The moist static energy and moisture at the top of the subcloud layer is taken to be same as that within the subcloud layer. A value of $\alpha_i = 0.3$ (the relaxation parameter) is used for all cloud-types. The thick dash-dot lines represent the observed estimates of $(Q_1 - Q_R)/c_p$ and $-Q_2/c_p$. The thick solid lines are for the convective heating and moistening rates for the RAS version 1. The thin solid lines are for the new RAS with linear entrainment case and no downdraft. The long dashed lines is for quadratic entrainment case without downdraft. The short dashed lines are for the case of quadratic entrainment with downdraft. The dotted lines are also for the same case but with the downdraft starting from the level of minimum moist static energy.

data from Cox and Griffith (1978), and surface fluxes and their vertical distribution estimated using NCEP boundary layer formulation. It should be pointed out that the model generated heating and moistening balance exactly when vertically integrated. However, this is not true for the observed estimate and therefore, one should be cautious in comparing the two. It is probably more accurate to assume that the temperature measurement is more reliable than the humidity measurement. Although there is some uncertainty in the radiation data, it is likely that the observed estimate of cumulus drying is too small.

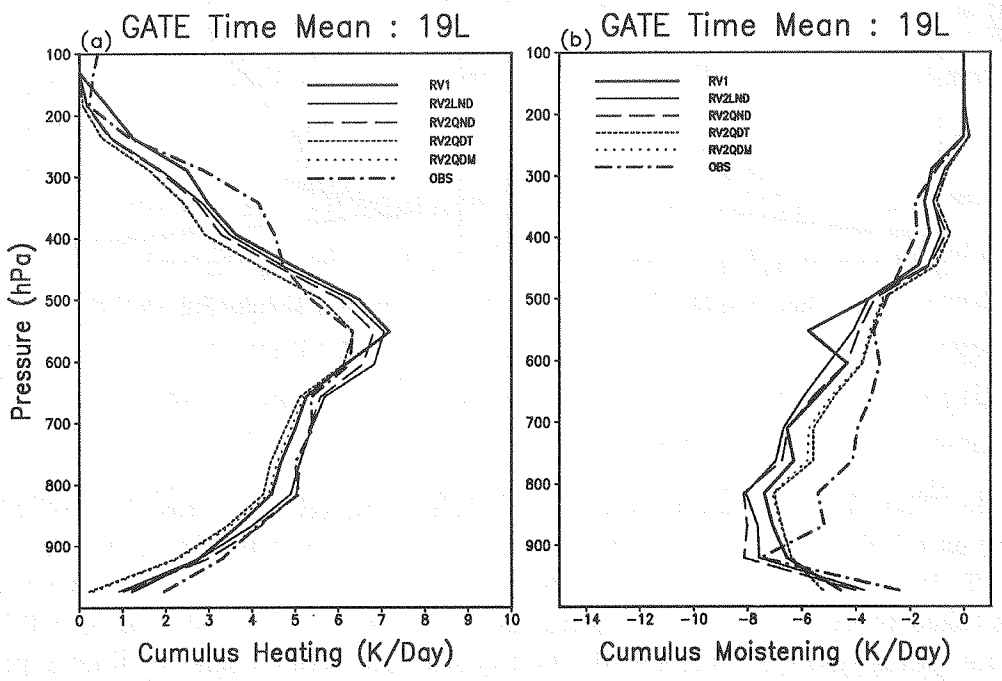


Figure 4: Same as in Fig. 3, but with the value of moist static energy and moisture at the subcloud layer top are taken as a mean of the corresponding values within the subcloud layer and the layer above.

From Fig. 3 we infer that RAS version 1 produces higher heating at virtually all levels

than the observed estimate. Cumulus drying is also larger than the observed estimate at almost all levels. RAS version 2 with linear entrainment produces very similar results with slightly more (less) heating at lower (upper) levels and slightly more (less) drying at lower (upper) levels. Inclusion of the quadratic entrainment relation changes the results only slightly. When the downdraft is included, the heating profile is closest to the observed profile below 400 hPa and cooler than observed above that level. Cumulus drying is clearly the lowest with the downdraft included. It should be remarked that the vertically integrated cumulus heating is very close to the observed estimate. Since the predicted heating exactly balances the predicted drying, the large difference we see in Fig. 3b between the observed estimate and predicted drying can only be interpreted as a consequence of uncertainty in the observed estimates.

Fig. 4a,b show GATE time mean convective heating and moistening rate for the second set of experiments. All lines in this figure correspond to the cases shown in in Fig. 3 but with direct modification of the subcloud layer by the cumulus subsidence. It is apparent that the results are substantially different. Essentially, the effect is to reduce the heating and drying, with RAS version 2 being slightly warmer and drier at lower levels and cooler and more moist at upper levels compared to RAS version 1. With downdraft, the new scheme produces heating rates similar to the old scheme at lower levels and lower heating rates at upper levels. Similarly, the drying rates are the lowest at almost all levels. From these results, we can conclude that the new RAS produces acceptable results. However, these semi-prognostic tests are insufficient to show whether the new RAS is significantly superior to the earlier version.

# 8 Application Strategy

Until now we have documented the methodology for calculating the modification of the environmental sounding due to a single cloud type. As stated before, in RAS we invoke one cloud type at time, letting each cloud type modify the environment partially. Thus over a reasonable time period, the destabilization due to the large-scale forcing and the stabilization due to the cumulus convection will be in quasi-equilibrium.

We generally represent a cloud type by the level of detrainment. In a model with $K$ layers, there can be, at most, $K-1$ cloud types with $k^{th}$ cloud type representing an ensemble of clouds detraining between pressure levels $p_{k+\frac{1}{2}}$ and $p_{k-\frac{1}{2}}$. A full spectrum would include all clouds detraining between the model top and the level of free convection. Then for a reasonably good representation of the full spectrum, we need to be able invoke all possible cloud types within a reasonable period.

When the number of model levels become large, the number of possible cloud types also becomes large. This implies that the cloud spectrum is divided into finer subensembles, and covering the full spectrum requires invoking more cloud types with a smaller relaxation parameter. This implies that the cost scales like the number of levels squared. We did not worry about this in the original RAS because it was fairly inexpensive and was being used in relatively coarse models. The new RAS, however, is computationally intensive and invoking too many cloud types can be prohibitively expensive. Furthermore, since the detrainment is assumed to occur only at the cloud top, having a too thin detrainment layer might result in strong moistening at the cloud top, and calling only a few "representative" clouds can result in very noisy profiles.

To overcome this problem, we have devised the following strategy. This is applicable when the vertical resolution of the model is high. This strategy is similar to viewing the cloud spectrum as a set of discrete $\Delta\lambda$'s. We can divide the pressure domain that represents the full spectrum of detrainment levels into a reasonable number of cloud types with a fairly thick layer of detrainment ($\approx$ 50 or 100 hPa). Then, using these pressure thickness as a guide, we strap one or more layers of a higher vertical resolution model to come up with a modified cloud spectrum which has somewhat thicker detrainment layers. We invoke several of these cloud types every time-step thus covering the full spectrum in a short time. Within each of the strapped layers the modification of the environment due to a given cloud type is assumed to be the same. Note that by doing this, the computational requirement scales linearly with vertical resolution.

To see how this strategy might work, we have applied it to the semi-prognostic test using an equally spaced, 40 layer version of the model with GATE data. In this test

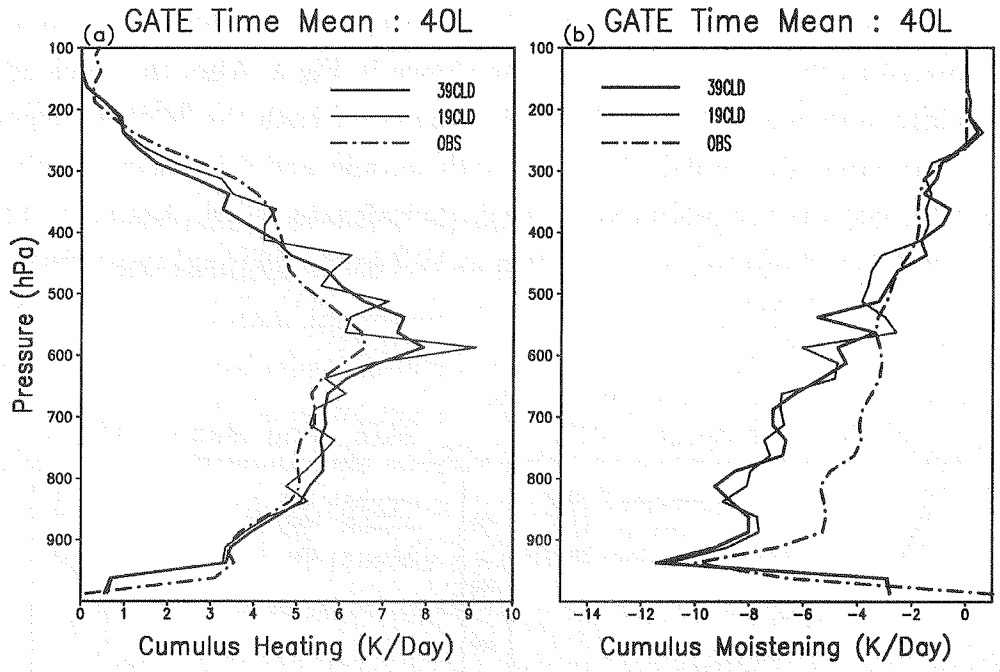


Figure 5: The time-averaged convective (a) heating (K/day) and (b) moistening (K/day) as a function of height obtained in the semi-prognostic test with 40 equally spaced vertical levels. In this case subcloud layer is modified by convection, but no downdraft is allowed. The thick dash-dot lines represent the observed estimates of $(Q_1 - Q_R)/c_p$ and $-Q_2/c_p$. The thick solid lines are for the convective heating and moistening rates when 39 cloud types are allowed. The thin solid lines are for the case with 19 cloud types having two strapped model layers as detrainment layers. A value of $\alpha_i = 0.05$ is used for the 39 cloud case and $\alpha_i = 0.1$ for the 19 cloud case.

the bottom two layers are considered as the subcloud layers. Figure 5 shows the time-averaged convective heating and moistening as a function of height obtained in this test without the downdraft. The thick solid lines are obtained using all of the 39 possible cloud types. The thin solid lines are obtained when only 19 cloud types with detrainment layer having two strapped model layers. The dash-dotted lines again show the observed estimate. Notice that the heating and moistening are somewhat noisy compared to the previous 19 level case shown in Fig.4. Also, the 19 cloud type case is slightly more noisy. Nevertheless, the results for both the 39 cloud types and 19 cloud types are quite similar. They are both warmer and drier than the observed estimate. Fig. 6 shows the results when the downdraft is included. Again, the profiles are quite similar for both the 39 cloud type as well as the 19 cloud type cases.

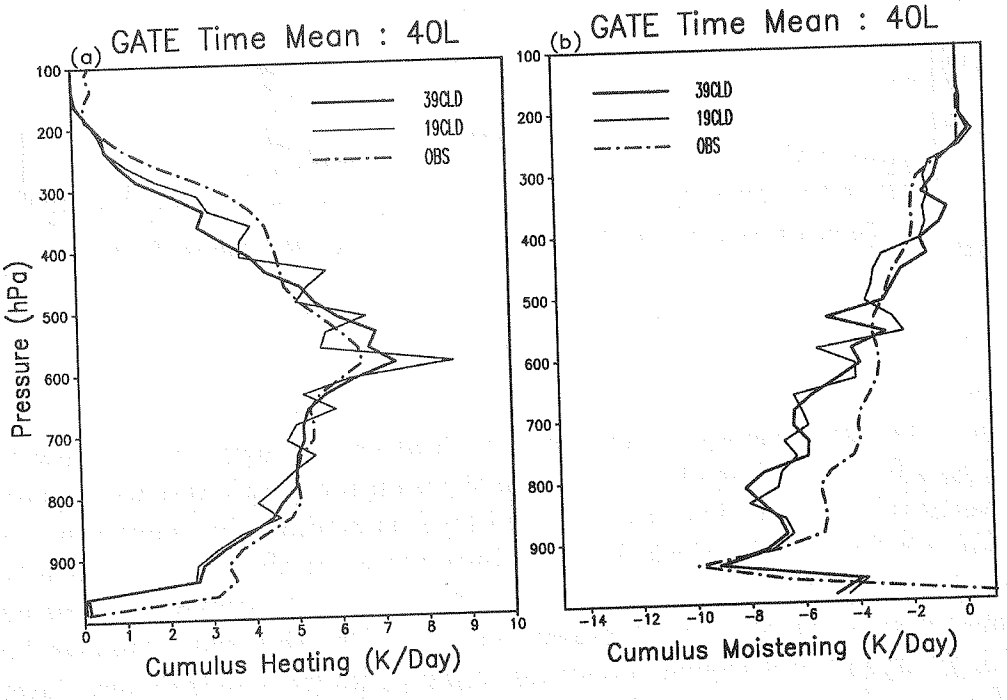


Figure 6: Same as in 5 but with downdraft included.

We have also applied the above strategy to a semi-Lagrangian global model (Moorthi, 1997) as well as the NCEP Global Spectral Model and the results are promising. Nevertheless, more work is needed to further assess whether this strategy is useful. Also, more work is needed in reducing the noise in the results with increased vertical resolution.

# 9 Summary

In this report we have provided a detailed documentation of an advanced version of the Relaxed Arakawa-Schubert convection parameterization. This version of RAS includes several important improvements over the original RAS. The cloud model now includes the virtual effects of moisture on buoyancy. It also includes condensate loading and takes into account the production of precipitation as the updraft ascends. Quadratic entrainment is an option that is included with minimal additional complexity. A crude representation of ice phase for the condensate is also included. Detrainment at the cloud top provides a source of cloud condensate for models having cloud condensate as a prognostic variable.

Following Cheng and Arakawa (1997a,b), we have also incorporated a simplified version of their evaporatively driven downdraft into this version of RAS. For computational reasons, we have chosen to fix the vertical tilt of the updraft for a given cloud type. Even so, the scheme is quite expensive. For further economy, we have provided an option in the code to start the downdraft calculation from any level of the model at or below the detrainment layer. Since RAS invokes one cloud type at a time, one can also economize by invoking downdrafts only for deep cloud types.

A scheme for evaporation of falling precipitation is also included, in addition to the evaporation within the downdraft. This is necessary to account for evaporation in the absence of the downdraft.

We have presented some results from semi-prognostic tests of this RAS with GATE data. Results showed that the performance of new RAS is similar to that of the

original RAS when the downdrafts are not included. It produces reasonably good (slightly larger) heating but excessive drying at lower levels. Inclusion of downdrafts reduces this low-level drying.

We have recently incorporated this RAS into a version of NCEP global spectral model. We are currently performing numerical simulation experiments to evaluate the performance of this version of RAS in climate simulations. Results from these experiments will be reported elsewhere.

An advantage of the new RAS over the old one is in providing a good estimate of the detrained cloud condensate. It also provides precipitation at all levels. This is an improvement over the original RAS in which the precipitation occurs only at the cloud top. In the earlier version we had to use a fraction of this precipitation at the cloud top as detrained cloud condensate. The new RAS removes the need for this arbitrariness. Also, with the precipitation falling from different heights, its evaporation in the environment can be expected to be more realistic compared to the way in which it is treated in the previous version (Moorthi 1999).

# Acknowledgements

We thank Professor A. Arakawa of UCLA and Dr. M.-D. Cheng of Central Weather Bureau, Taiwan for their help in understanding their downdraft formulation. We thank Dr. S. Lord and Professor E. Kalnay for providing encouragement during this work. Furthermore, we thank Mr. R. Kistler and Dr. K. Mitchell for excellent NCEP internal review of this manuscript. We also thank Ms. Joyce Peters for making arrangement for publication of this NOAA Technical Report.

# Appendix A

### Derivation of the quadratic equation for the entrainment parameter

In this appendix we provide a more detailed derivation of the quadratic equation for the entrainment parameter. From (25) using (8), we have

$$\eta^u_{k-\frac{1}{2}} q^u_{k-\frac{1}{2}} = \eta^u_{k-\frac{1}{2}} q^*_{k-\frac{1}{2}} + \frac{\gamma_{k-\frac{1}{2}}}{L_c(1+\gamma_{k-\frac{1}{2}})} \eta^u_{k-\frac{1}{2}} \left( h^u_{k-\frac{1}{2}} + L_f Q_{k-\frac{1}{2}} - h^*_{k-\frac{1}{2}} \right). \tag{92}$$

Using (74) and (60) in (92), we can write

$$\eta^u_{k-\frac{1}{2}} q^u_{k-\frac{1}{2}} = C_{k-\frac{1}{2}} + \lambda D_{k-\frac{1}{2}} + \lambda^2 E_{k-\frac{1}{2}} + \frac{\gamma_{k-\frac{1}{2}}}{L_c(1+\gamma_{k-\frac{1}{2}})} \eta^u_{k-\frac{1}{2}} L_f Q_{k-\frac{1}{2}}, \tag{93}$$

where

$$C_{k-\frac{1}{2}} = q^*_{k-\frac{1}{2}} - \frac{\gamma_{k-\frac{1}{2}}}{L_c(1+\gamma_{k-\frac{1}{2}})} \left( h^*_{k-\frac{1}{2}} - h_K \right), \tag{94a}$$

$$\begin{aligned} D_{k-\frac{1}{2}} &= \zeta_{k-\frac{1}{2}} \left[ q^*_{k-\frac{1}{2}} - \frac{\gamma_{k-\frac{1}{2}}}{L_c(1+\gamma_{k-\frac{1}{2}})} h^*_{k-\frac{1}{2}} \right] \\ &+ \frac{\gamma_{k-\frac{1}{2}}}{L_c(1+\gamma_{k-\frac{1}{2}})} \sum_{K-1}^{k} \left( \zeta_{j-\frac{1}{2}} - \zeta_{j+\frac{1}{2}} \right) h_j, \end{aligned} \tag{94b}$$

$$\begin{aligned} E_{k-\frac{1}{2}} &= \xi_{k-\frac{1}{2}} \left[ q^*_{k-\frac{1}{2}} - \frac{\gamma_{k-\frac{1}{2}}}{L_c(1+\gamma_{k-\frac{1}{2}})} h^*_{k-\frac{1}{2}} \right] \\ &+ \frac{\gamma_{k-\frac{1}{2}}}{L_c(1+\gamma_{k-\frac{1}{2}})} \sum_{K-1}^{k} \left( \xi_{j-\frac{1}{2}} - \xi_{j+\frac{1}{2}} \right) h_j. \end{aligned} \tag{94c}$$

Substituting (93) into (70) we obtain

$$a'_k \eta^u_{k-\frac{1}{2}} q^{uC}_{k-\frac{1}{2}} = b'_k \eta^u_{k+\frac{1}{2}} q^{uC}_{k+\frac{1}{2}} + F_k + \lambda G_k + \lambda^2 H_k, \tag{95}$$

where

$$a'_k = a_k + \frac{\gamma_{k-\frac{1}{2}}}{L_c(1+\gamma_{k-\frac{1}{2}})} L_f Q_{k-\frac{1}{2}}, \tag{96a}$$

$$b'_k = b_k + \frac{\gamma_{k+\frac{1}{2}}}{L_c(1+\gamma_{k+\frac{1}{2}})} L_f Q_{k+\frac{1}{2}}, \tag{96b}$$

$$F_k = C_{k+\frac{1}{2}} - C_{k-\frac{1}{2}}, \tag{96c}$$

$$G_k = D_{k+\frac{1}{2}} - D_{k-\frac{1}{2}} - q_k^T \left(\zeta_{k-\frac{1}{2}} - \zeta_{k+\frac{1}{2}}\right), \tag{96d}$$

$$H_k = E_{k+\frac{1}{2}} - E_{k-\frac{1}{2}} - q_k^T \left(\xi_{k-\frac{1}{2}} - \xi_{k+\frac{1}{2}}\right). \tag{96e}$$

Similarly, at the cloud top we can obtain

$$a'_i \eta_i^u q_i^{uC} = b'_i \eta_{i+\frac{1}{2}}^u q_{i+\frac{1}{2}}^{uC} + F_i + \lambda G_i + \lambda^2 H_i. \tag{97}$$

Using (95) in (97), we can finally write the following expression for the total condensate at the cloud top:

$$\eta_i^u q_i^{uC} = \tilde{F}_i + \lambda \tilde{G}_i + \lambda^2 \tilde{H}_i, \tag{98}$$

where

$$\tilde{F} = \frac{1}{a'_i}\left[F_i + \frac{b'_i}{a_{i+1}}\left(F_{i+2} + \ldots + \frac{b'_{K-2}}{a_{K-1}} F_{K-1}\right)\right], \tag{99a}$$

$$\tilde{G} = \frac{1}{a'_i}\left[G_i + \frac{b'_i}{a'_{i+1}}\left(G_{i+2} + \ldots + \frac{b'_{K-2}}{a_{K-1}} G_{K-1}\right)\right], \tag{99b}$$

$$\tilde{H} = \frac{1}{a'_i}\left[H_i + \frac{b'_i}{a'_{i+1}}\left(H_{i+2} + \ldots + \frac{b'_{K-2}}{a_{K-1}} H_{K-1}\right)\right]. \tag{99c}$$

From the non-buoyancy condition (35) applicable at the cloud top $i$, and using (98), (8) and (74), we can obtain a quadratic equation in $\lambda$ as

$$a\lambda^2 + b\lambda + c = 0 \tag{100}$$

where

$$a = \sum_{K-1}^{i+1} (\xi_{j-\frac{1}{2}} - \xi_{j+\frac{1}{2}}) h_j + (\xi_i - \xi_{i+\frac{1}{2}}) h_i - \xi_i h^{**} - (\tilde{L}_i - L_f Q_i)\tilde{H}, \tag{101a}$$

$$b = \sum_{K-1}^{i+1} (\zeta_{j-\frac{1}{2}} - \zeta_{j+\frac{1}{2}}) h_j + (\zeta_i - \zeta_{i+\frac{1}{2}}) h_i - \zeta_i h^{**} - (\tilde{L}_i - L_f Q_i)\tilde{G}, \tag{101b}$$

and

$$c = h_K - h^{**} - (\tilde{L}_i - L_f Q_i)\tilde{F}. \tag{101c}$$

The quadratic equation (100) has real solutions when $b^2 - 4ac > 0$. Only when a real solution is positive, such an updraft can exist. If both solutions are positive, we select the one with larger positive value if that value does not exceed an imposed upper limit on $\lambda$.

# Appendix B

### Evaporation of falling precipitation in the environment

In this appendix we document the way in which Sud and Molod (1988) scheme for evaporation of falling convective precipitation is used in RAS. Following Sud and Molod, we parameterize the fraction of the precipitation that is evaporated into the environment in layer $k$ at or below the updraft detrainment level $i$ as (See Moorthi, 1999)

$$f_k = Min\{1, \frac{\Delta q}{P_r}\sigma_k[P_r(3600/\Delta t)(p/1000)^{0.5}]^{0.578}\}, \tag{102}$$

where $\Delta q$ is the saturation moisture deficit of that layer calculated iteratively (we use three iterations), $P_r$ is the precipitation over a time-step of $\Delta t$ seconds that is available for evaporation, and $p$ is the pressure at the middle of the layer in $hPa$. Here, $\sigma_k$ is the horizontal fractional area of the grid covered by the falling convective precipitation. The value of $\sigma_k$ can be between 0 and 1. Currently, we parameterize $\sigma_k$ as

$$\sigma_k = Min\{1, \mathcal{W}_k g M_B \eta_i / \Delta p_i\} \tag{103}$$

where $\mathcal{W}_k$ is a tuning parameter, $M_B$ is the cloud-base mass flux, $\eta_i$ is normalized mass flux at the cloud top, and $\Delta p_i$ is the pressure thickness of the detrainment layer, $g$ is the gravitational acceleration, and $k = i, i+1, \ldots, K+M-1$ where $K+M-1$ is the total number of model layers. Although we have allowed $\mathcal{W}_k$ in (103) to be a function of height, in our experiments we have used a constant value for all levels.

# REFERENCES


Arakawa, A., and W. H. Schubert, 1974: Interaction of a cumulus cloud ensemble with the large-scale environment. Part I. *J. Atmos. Sci..*, **31**, 674-701.

Arakawa, A., and M.-D. Cheng, 1993: The Arakawa-Schubert cumulus parameterization *The representation of cumulus convection in numerical models of the atmosphere*, K. A. Emanuel and D. J. Raymond, Ed. American Meteorological Society, 123-136.

Cheng, M.-D., 1989: Effects of downdrafts and mesoscale convective organization on the heat and moisture budgets of tropical cloud clusters. Part I: A diagnostic cumulus ensemble model. *J. Atmos. Sci..*, **46**, 1517-1538.

Cheng, M.-D., and A. Arakawa, 1997a: Inclusion of rain water budget and convective downdrafts in the Arakawa-Schubert cumulus parameterization. *J. Atmos. Sci..*, **54**, 1359-1378.

Cheng, M.-D., and A. Arakawa, 1997b: Computational procedures for the Arakawa-Schubert cumulus parameterization: Tech. Rep. No. 101, Department of Atmospheric Sciences, University of California, Los Angeles, pp 50.

Cox, S. K., and K. T. Griffith, 1978: Tropospheric radiative divergence during Phase III of GARP Atlantic Tropical Experiment (GATE). Atmos. Sci. Paper No.291 Colorado State University, 166pp.

Hong, S-Y., and H. L. Pan, 1996: Nonlocal boundary layer vertical diffusion in a medium-range forecast model. *Mon. Wea. Rev..*, **124**, 2322-2339.

Kao, C. Y. J., and Y. Ogura, 1987: Response of cumulus clouds to large-scale forcing using the Arakawa-Schubert cumulus parameterization. *J. Atmos. Sci..*, **44**, 2437-2458.

Krishnamurti, T. N., Y. Ramanathan, H.-L. Pan, R. J. Pasch, and J. Molinari, 1980: Cumulus parameterization and rainfall rates I. *Mon. Wea. Rev..*, **108**, 465-

472.

Lord, S. J., 1978: Development and observational verification of a cumulus cloud parameterization. Ph.D. dissertation, University of California, Los Angeles, 359 pp.

Lord, S. J., 1982: Interaction of a cumulus cloud ensemble with the large-scale environment. Part III: Semiprognostic test of the Arakawa-Schubert cumulus parameterization. *J. Atmos. Sci..*, **39**, 88-103.

Lord, S. J., W. C. Chao, and A. Arakawa, 1982: Interaction of a cumulus cloud ensemble with the large-scale environment. Part IV: The discrete model. *J. Atmos. Sci..*, **39**, 104-113.

Moorthi, S., 1997: NWP experiments with a semi-Lagrangian semi-implicit global model at NCEP. *Mon. Wea. Rev..*, **120**, 978-1002.

Moorthi, S., 1999: Application of Relaxed Arakawa-Schubert cumulus parameterization to the NCEP climate model - some sensitivity experiments. *General Circulation Modeling: Past, Present and Future*, Ed. David Randall, Publisher: Academic Press.

Moorthi, S., and M.J. Suarez, 1992: Relaxed Arakawa-Schubert: A parameterization of moist convection for general circulation models. *Mon. Wea. Rev..*, **120**, 978-1002.

Simpson, J. and V. Wiggert, 1969: Models of precipitating cumulus towers. *Mon. Wea. Rev..*, **97**, 471-489.

Sud, Y., and A. Mood, 1988: The roles of dry convection, cloud-radiation feedback processes, and the influence of recent improvements in the parameterization of convection in the GLA GCM. *Mon. Wea. Rev..*, **116**, 2366-2387.

Sud, Y., and G. K. Walker, 1999a: Microphysics of clouds with the relaxed Arakawa-Schubert Scheme (McRAS). Part I: Design and evaluation with GATE Phase III data. *J. Atmos. Sci..*, (In press).

Sud, Y., and G. K. Walker, 1999b: Microphysics of clouds with the relaxed Arakawa-Schubert Scheme (McRAS). Part I: Implementation and performance in GEOS II GCM. *J. Atmos. Sci..*, (In press).

Thompson R. M., Jr., S. W. Payne, E. E. Recker, and R. J. Reed, 1979: Structure and properties of synoptic-scale wave disturbances in the intertropical convergence zone of the eastern Atlantic. *J. Atmos. Sci..*, **36**, 53-72.

Yanai, M., S. K. Esbensen, and J. H. Chu, 1973: Determination of bulk properties of tropical cloud clusters from large-scale heat and moisture budgets. *J. Atmos. Sci..*, **30**, 611-627.

## NOAA SCIENTIFIC AND TECHNICAL PUBLICATIONS

The National Oceanic and Atmospheric Administration was established as part of the Department of Commerce on October 3, 1970. The mission responsibilities of NOAA are to assess the socioeconomic impact of natural and technological changes in the environment and to monitor and predict the state of the solid Earth, the oceans and their living resources, the atmosphere, and the space environment of the Earth.

The major components of NOAA regularly produce various types of scientific and technical information in the following kinds of publications:

PROFESSIONAL PAPERS - Important definitive research results, major techniques, and special investigations.

CONTRACT AND GRANT REPORTS - Reports prepared by contractors or grantees under NOAA sponsorship.

ATLAS - Presentation of analyzed data generally in the form of maps showing distribution of rainfall, chemical and physical conditions of oceans and atmosphere, distribution of fishes and marine mammals, ionospheric conditions, etc.

TECHNICAL SERVICE PUBLICATIONS - Reports containing data, observations, instructions, etc. A partial listing includes data serials; prediction and outlook periodicals; technical manuals, training papers, planning reports, and information serials; and miscellaneous technical publications.

TECHNICAL REPORTS - Journal quality with extensive details, mathematical developments, or data listings.

TECHNICAL MEMORANDUMS - Reports of preliminary, partial, or negative research or technology results, interim instructions, and the like.